Eur. Phys. J. D **35**, 499–503 (2005)
DOI: 10.1140/epjd/e2005-00080-2

THE EUROPEAN PHYSICAL JOURNAL D

Triple differential cross-section for the ionization of H^- at low energies

R.K. Chauhan[1,a], M.K. Srivastava[2,b], and R. Srivastava[1,c]

[1] Department of Physics, Indian Institute of Technology, Roorkee-247 667, India
[2] Institute Instrumentation Centre, Indian Institute of Technology, Roorkee-247 667, India

Received 26 February 2005 / Received in final form 5 April 2005
Published online 7 June 2005 –

Abstract. The triple differential cross-sections (TDCS) for the ionization of H^- at excess energies of 8, 10 and 12 eV are calculated using distorted-wave Born approximation in the equal energy sharing and $\theta_{ab} = 180^\circ$ kinematics. The final state electron-electron correlation is included through effective charges and exchange distortion in semi-classical local approximation. The spin state of the exchanging electrons is taken care of. The angular distribution of the TDCS is very different from the case of helium and is found to show peaks at $\theta_a \approx 30^\circ$ and 150°. The capture process is found to contribute quite significantly around $\theta_a = 90^\circ$ and is supported by the PCI.

PACS. 34.80.Dp Atomic excitation and ionization by electron impact

1 Introduction

The interest in the study of $(e, 2e)$ process close to ionization threshold grew since the experiments of Selles et al. [1] and Schlemmer et al. [2] on hydrogen and helium about fifteen years ago. The experiments were later performed on neon, argon, krypton and xenon [3,4]. It is found that the triple differential cross-sections (TDCS) are very sensitive to target-dependent short-range correlations and lead to different angular distributions at low energies even though at asymptotic separations the long-range interactions in the final state are essentially identical. The spectacular difference in the angular distribution of TDCS close to threshold with respect to the angle θ_a of emission of one of the electrons in equal energy sharing ($E_a = E_b$) and $\theta_{ab} = 180^\circ$ geometry for hydrogen and helium is a manifestation of this aspect [2]. The differences in the angular distribution are also found in the case of other inert gas targets. Several calculations have been done to understand the dynamics of ionization close to threshold. These were done (i) with emphasis on asymptotically correct three-body Coulomb boundary conditions [5–10], (ii) in convergent close-coupling approximation [11–16], (iii) in exterior complex scaling method [17–19], (iv) in quantal-semiclassical treatment [20,21], (v) in hyperspherical R-matrix approach [22,23], (vi) in time-dependent approach [24,25] and (vii) in distorted-wave Born approximation (DWBA) [26–38]. Of these DWBA has been quite successful and widely used. It is essentially a high energy approximation but has been extended to lower energies by appropriately incorporating into it post-collision interaction, exchange distortion and target polarization effects which are very important at low energies. Helium has been quite widely used as a target for these studies. In the present work we consider $(e, 2e)$ process on H^- ion at low energies. It differs from the corresponding helium case in the sense that (i) in the initial channel the electron–target static potential changes sign, negative near the target and positive at large distance and (ii) the final channel does not have three charged particles. This study is interesting because of the following reasons: (i) very low binding energy of H^- (0.762 eV) as compared to 24.6 eV of helium. This is expected to enhance the effect of short-range electron-electron correlation on the TDCS. This may also have influence on the capture process where projectile electron is captured by the target and both the target electrons are ejected. (ii) Large dipole polarizability of the target.

In the present work the calculation of TDCS has been done using DWBA. The exchange distortion has been included by using semi-classical local exchange potential of Furness and McCarthy [39] as corrected by Gianturco and Scialla [40]. It is found to be quite reasonable even at low energies. In particular, when the ionization of the atom is from an s-state [41–43]. In constructing the distortion potentials in the initial and final channels, the spin-state of the exchanging electrons has been taken care of. For example, in the initial channel, exchange is possible only with one of the target electrons as the H^- ground state is

[a] e-mail: rajkrdph@iitr.ernet.in
[b] e-mail: mksrific@iitr.ernet.in
[c] e-mail: rajsrfph@iitr.ernet.in

spin-singlet and the exchanging electrons are therefore in the spin-triplet state. The situation in the final channel is a little more involved. In the case of triplet scattering amplitudes (direct f_t and exchange g_t), the exchange distortion potential is spin-singlet for both the scattered and ejected electrons 'a' and 'b'. However for singlet scattering amplitudes (f_s, g_s and capture h_s), the exchange distortion potential in spin-singlet for one electron and spin–triplet for the other.

We consider next, the incorporation of post collision interaction (PCI) in the calculation. The use of Gamow factor to include PCI is found to lead to some over all improvement in DWBA results at incident energies above about 100 eV. Another approach, which is found to be quite good and has also been used in the present work is the use of effective charges to mimic PCI. These effective charges have been obtained in different ways, which satisfy certain limiting conditions (see for example Jetzke et al. [44–46] and the Rudge-Seaton-Peterkop relation [47] which is based upon the total interaction of three charged particles. Pan and Starace [26,27] have replaced the Coulomb interaction between the two continuum electrons by a variationally determined screening potential satisfying Rudge-Seaton-Peterkop relation. Jones et al. [28] in their study close to ionization threshold have used the physical argument that each of the effective charges contains the interaction with the other electron and have obtained

$$Z_a = Z_b = 1 - \frac{1}{2\sin\left(\frac{\theta_{ab}}{2}\right)} \tag{1}$$

for equal energy final state electrons 'a' and 'b'. Here θ_{ab} is their angular separation. This choice ensures a vanishingly small cross-section as the angular separation goes to zero. It should however be noted that any model using angle-dependent effective charges shall lead to non-physical result that the effective charge vanishes whenever the contribution representing electron-nucleus interaction cancels the contribution representing electron-electron interaction. This is because these effective charges lead to radial force on the electrons where as in the final state comprising of three charged particles, the force on the electrons is not radial. However, in $\theta_{ab} = 180^\circ$ geometry, this approach does not suffer from this drawback as the interactions between all the particles in the final state are radial. The asymptotic effective charges Z_a and Z_b for equal energy final state ($E_a = E_b$) and $\theta_{ab} = 180^\circ$ are given by

$$Z_a = Z_b = 1 - \frac{1}{2} = \frac{1}{2}. \tag{2}$$

The calculation has been done at excess energy E_{ex} (= incident energy E_i – ionization potential I) ≤ 12 eV in $\theta_{ab} = 180^\circ$ geometry. This low energy region is known to be appropriate to study the effect of short-range correlations. As the incident energy increases the angular distribution of TDCS tends to become qualitatively identical. The geometry $\theta_{ab} = 180^\circ$ has been chosen because the differences in the angular distribution of TDCS are most spectacular here. The effective charge model used here is also most appropriate in this geometry.

The details of the calculation are given in Section 2. The results are presented in Section 3. Some concluding remarks made in Section 4.

2 Theory

The TDCS for the single ionization of H^- by electrons with energy E_i (momentum $\boldsymbol{k}_i$) can be defined as follows (Atomic units have been used throughout):

$$\frac{d^3\sigma}{dE_b d\Omega_a d\Omega_b} = (2\pi)^4 \frac{k_a k_b}{k_i} \times \left(\frac{3}{2}\left|f_t - g_t\right|^2 - \frac{1}{2}\left|f_s - g_s\right|^2 + \left|h_s - f_s\right|^2 + \left|h_s - g_s\right|^2\right). \tag{3}$$

Here f, g and h are direct, exchange and capture amplitudes for triplet (t) and singlet (s) scattering. In case the singlet/triplet scattering is not differentiated, the above equation reduces to

$$\frac{d^3\sigma}{dE_b d\Omega_a d\Omega_b} = (2\pi)^4 \frac{k_a k_b}{k_i} \times \left(\left|f - g\right|^2 + \left|h - f\right|^2 + \left|h - g\right|^2\right). \tag{4}$$

If, on the other hand, the capture amplitude h is dropped,

$$\frac{d^3\sigma}{dE_b d\Omega_a d\Omega_b} = (2\pi)^4 \frac{k_a k_b}{k_i} \left(\frac{3}{2}\left|f_t - g_t\right|^2 + \frac{1}{2}\left|f_s + g_s\right|^2\right). \tag{5}$$

The amplitudes f, g and h are given by

$$f = \left\langle \chi_a^{(-)}(\boldsymbol{r}_0)\xi_{b,f}(\boldsymbol{r}_1,\boldsymbol{r}_2)\left|\frac{1}{r_{01}} + \frac{1}{r_{02}}\right|\psi_i(\boldsymbol{r}_1,\boldsymbol{r}_2)\chi_i^{(+)}(\boldsymbol{r}_0)\right\rangle, \tag{6}$$

$$g = \left\langle \chi_b^{(-)}(\boldsymbol{r}_0)\xi_{a,f}(\boldsymbol{r}_1,\boldsymbol{r}_2)\left|\frac{1}{r_{01}} + \frac{1}{r_{02}}\right|\psi_i(\boldsymbol{r}_1,\boldsymbol{r}_2)\chi_i^{(+)}(\boldsymbol{r}_0)\right\rangle, \tag{7}$$

$$h = \left\langle \psi_f(\boldsymbol{r}_0)\zeta_{a,b}(\boldsymbol{r}_1,\boldsymbol{r}_2)\left|\frac{1}{\boldsymbol{r}_{01}} + \frac{1}{\boldsymbol{r}_{02}}\right|\psi_i(\boldsymbol{r}_1,\boldsymbol{r}_2)\chi_i^{(+)}(\boldsymbol{r}_0)\right\rangle. \tag{8}$$

The final state wave functions $\xi(\boldsymbol{r}_1,\boldsymbol{r}_2)$ and $\zeta(\boldsymbol{r}_1,\boldsymbol{r}_2)$ of the target are Schmidt orthogonalized to the target initial state wavefunction $\psi_i(\boldsymbol{r}_1,\boldsymbol{r}_2)$

$$\xi_{a,f}(\boldsymbol{r}_1,\boldsymbol{r}_2) = \chi_a^{(-)}(\boldsymbol{r}_1)\psi_f(\boldsymbol{r}_2) - \left\langle \psi_i(\boldsymbol{r}_1',\boldsymbol{r}_2')\middle|\chi_a^{(-)}(\boldsymbol{r}_1')\psi_f(\boldsymbol{r}_2')\right\rangle \psi_i(\boldsymbol{r}_1,\boldsymbol{r}_2), \tag{9}$$

$$\zeta_{a,b}(\boldsymbol{r}_1,\boldsymbol{r}_2) = \chi_a^{(-)}(\boldsymbol{r}_1)\chi_b^{(-)}(\boldsymbol{r}_2) - \left\langle \psi_i(\boldsymbol{r}_1',\boldsymbol{r}_2')\middle|\chi_a^{(-)}(\boldsymbol{r}_1')\chi_b^{(-)}(\boldsymbol{r}_2')\right\rangle \psi_i(\boldsymbol{r}_1,\boldsymbol{r}_2). \tag{10}$$

Here $\chi_a^{(-)}$ and $\chi_b^{(-)}$ are normalized final state distorted waves of the two outgoing electrons 'a' and 'b' having energies E_a and E_b and momenta $\boldsymbol{k}_a$ and $\boldsymbol{k}_b$ respectively. These are eigenfunction of the distorting potentials U_{af} and U_{bf}. The distorted wave for the incident electron, $\chi_i^{(+)}$, is normalized eigenfunction of the initial state distorting potential $U_i(r)$ and $\psi_i(\boldsymbol{r}_1, \boldsymbol{r}_2)$ is the initial state wave function of H^-. It is given by [48] where

$$\psi_i(\boldsymbol{r}_1, \boldsymbol{r}_2) = N_0(e^{-\eta_1 r_1} e^{-\eta_2 r_2} + e^{-\eta_1 r_2} e^{-\eta_2 r_1}), \quad (11)$$

$$N_0 = 0.3948/4\pi, \quad \eta_1 = 1.0392, \quad \eta_2 = 0.2832.$$

The wave function $\psi_f(\boldsymbol{r})$ in equations (8) and (9) is the wave function of the residual hydrogen atom and $\boldsymbol{r}_0$, $\boldsymbol{r}_1$ and $\boldsymbol{r}_2$ are respectively the position vectors of the projectile electron and the electrons of the target with respect to the target nucleus. The energies are related by the conservation relation

$$E_i = I + E_a + E_b, \quad (12)$$

where I (= 0.762 eV) is the ionization potential of the target. Because of the orthogonalization of the final state wave function to the initial state wave function $\psi_i(\boldsymbol{r}_1, \boldsymbol{r}_2)$, equations (9) and (10), the distorting potentials do not contribute in the matrix elements, equations (6–8), and have therefore been dropped from the interaction there in.

The initial state distorting potential $U_i(r)$ is the sum of the static potential $U_{atom}(r_0)$ of H^-

$$U_{atom}(r_0) = \iint |\psi_i(\boldsymbol{r}_1, \boldsymbol{r}_2)|^2 \left(\frac{1}{r_{01}} + \frac{1}{r_{02}} - \frac{1}{r_0}\right) d\boldsymbol{r}_1 d\boldsymbol{r}_2 \quad (13)$$

as felt by the incident electron , semi-classical local exchange potential $U_{exchi}(r)$ [39,40]

$$U_{exchi}(r) = \frac{1}{2}\left[\left\{E_i - U_{atom} + \frac{3}{10}\Big(3\pi^2\rho_i(r)\Big)^{2/3}\right\} - \left\{\left\{E_i - U_{atom} + \frac{3}{10}\Big(3\pi^2\rho_i(r)\Big)^{2/3}\right\}^2 + 4\pi\rho_i(r)\right\}^{1/2}\right], \quad (14)$$

where

$$\rho_i(r) = \left[\frac{2}{(2\eta_1)^3}\exp(-2\eta_2 r) + \frac{2}{(2\eta_2)^3}\exp(-2\eta_1 r) + \frac{4}{(\eta_1+\eta_2)^3}\exp\Big(-(\eta_1+\eta_2)r\Big)\right] \quad (15)$$

and dipole polarization potential $U_{poli}(r)$ given by

$$U_{poli}(r) = -\frac{\alpha_d r^2}{(r^2+d^2)^3}, \quad (16)$$

where $\alpha_d = 206.149$ (a.u.) and

$$d = \frac{\eta_1 + \eta_2}{2\eta_1\eta_2}. \quad (17)$$

The final state electron-electron interaction is incorporated following Jones et al. [28] through the use of effective charges Z_a and Z_b which, for equal energy sharing are given by equation (1). The direct distorting potentials U_a and U_b are made to satisfy the following limiting physical conditions as in [28]

$$U_a(r) \to \begin{cases} -Z_a/r & \text{as} \quad r \to \infty \\ -Z/r & \text{as} \quad r \to 0 \end{cases} \quad (18)$$

$$U_a(r) \equiv U_b(r) \quad (19)$$

by using the combination

$$U_a(r) = Z_a U_H(r) + (1 - Z_a) U_{atom}(r) \quad (20)$$

where $U_H(r)$ is the static potential of the residual hydrogen atom

$$U_H(r) = -\Big(1 + \frac{1}{r}\Big)\exp(-2r). \quad (21)$$

These distorting potentials in the final channel have been constructed differently than the distortion potential in the initial channel as they need to satisfy the conditions at close encounter as well as mimic PCI.

The polarization potential $U_{polf}(r)$ given by

$$U_{polf}(r) = -\frac{4.5}{r^4}\left(1 - \left(1 + 2r + 2r^2 + \frac{4}{3}r^3 + \frac{2}{3}r^4 + \frac{4}{27}r^5\right)\exp(-2r)\right) \quad (22)$$

and the exchange potential $U_{exchf}(r)$ given by

$$U_{exchf}^{(S)}(r) = (-1)^{(S+1)}\frac{1}{2}\left[\left\{E - V + \frac{3}{10}\Big(3\pi^2\rho_f(r)\Big)^{2/3}\right\} - \left\{\left\{E - V + \frac{3}{10}\Big(3\pi^2\rho_f(r)\Big)^{2/3}\right\}^2 + 4\pi\rho_f(r)\right\}^{\frac{1}{2}}\right] \quad (23)$$

where

$$p_f(r) = 4\exp(-2r) \quad (24)$$

are then added to U_a (and U_b) with $V = U_a$ or U_b, $E = E_a$ or E_b, and $S = 0(1)$ to obtain U_{af} and U_{bf} for singlet (triplet) scattering amplitude.

Finally the scattering amplitudes f, g and h are simplified by using the usual partial wave expansion for distorted waves and angular momentum algebra [33] in equations (6–8) and the TDCS are finally obtained.

3 Results and discussion

We have calculated the TDCS at E_{ex} = 8, 10 and 12 eV in equal energy sharing and $\theta_{ab} = 180°$ geometry. In order to assess the contribution of capture process as well as

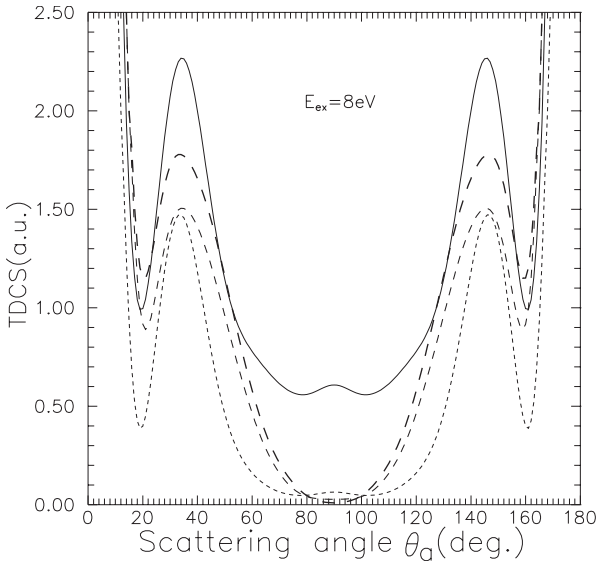

Fig. 1. Triple differential cross-sections (in a.u.) for the ionization of H^- in coplanar symmetric geometry with equal energy sharing ($E_a = E_b$) and $\theta_{ab} = 180°$ plotted against scattering angle θ_a at excess energy $E_{ex} = 8$. Results: ——— DW.CP.PCI, ------ DW.PCI, – – – – – DW.CP, – – – – – DW.

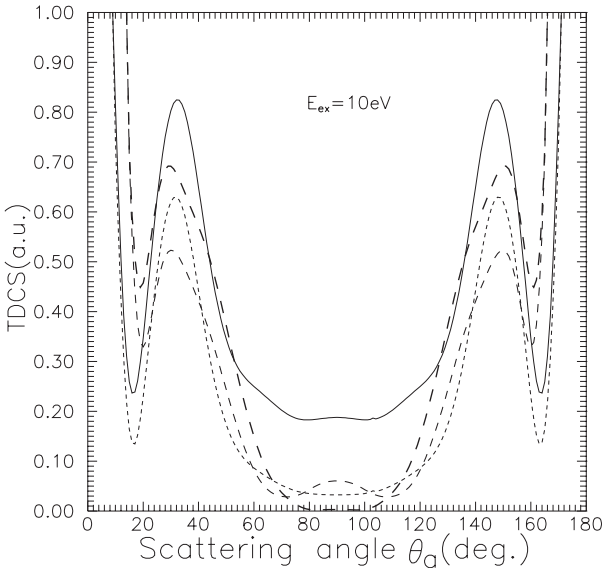

Fig. 2. Same as Figure 1, but at $E_{ex} = 10$ eV.

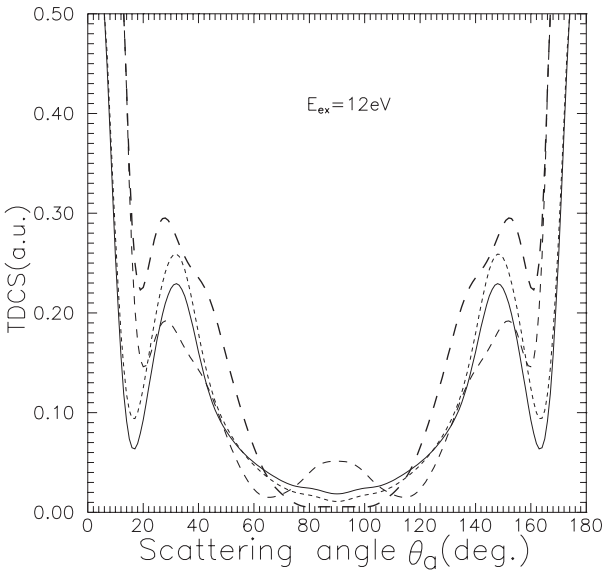

Fig. 3. Same as Figure 1, but at $E_{ex} = 12$ eV.

the effect of PCI we have performed four different types of calculations: (i) DW.CP.PCI- using equation (3) for the TDCS in which capture term is included along with the choice for U_a and U_b as given by equation (20) which includes PCI. (ii) DW.PCI- using equation (5) for TDCS which does not include capture contribution but PCI is included as in (i). (iii) DW.CP- using equation (3) for TDCS but switching off the PCI i.e. by replacing the final state distorting potential as taken in equation (20) by

$$U_a(r) = U_H(r) \tag{25}$$

and (iv) DW- using equation (5) for the TDCS and equation (25) for the final state distorting potentials, thus both capture contribution and the PCI are excluded in this calculation.

Figures 1–3 show our TDCS results respectively at $E_{ex} = 8$, 10 and 12 eV. In each figure we have shown all the four different types of calculations. In general from these three figures we find that the angular distribution of TDCS shows more structure than what is seen in the case of helium in all the four types of calculation considered here [2]. There are peaks in the cross-section curves at $\theta_a \approx 30°$ and 150°. This may be due to large spatial extent of H^- wave function.

Let us first consider the DW.CP.PCI results which include both the capture process and the PCI. The capture contribution is very important at low energies. We find that it contributes quite substantially around $\theta_a \approx 90°$ i.e. when the two final-state electrons are coming out symmetrically with respect to each other. This situation is naturally very appropriate for this process where the two initially bound electrons are coming out with equal energies. There is a low maximum in TDCS at $\theta_a = 90°$. Further a comparison of DW.CP.PCI and DW.PCI results shows that at $E_a = E_b = 4$ eV [Fig. 1], the dropping of capture contribution decreases the TDCS from 0.61 a.u. to 0.064 a.u. at $\theta_a = 90°$. As the energy increases this contribution falls of rapidly. For example, at $E_a = E_b = 6$ eV, the exclusion of capture process decreases the value of TDCS from its value of 0.019 a.u. to 0.011 a.u. only [see DW.CP.PCI and DW.PCI results in Fig. 3]. Such a strong contribution of the capture process as found for H^- is not found in the case of helium [28]. We believe that this feature is caused by the fact that H^- is a very loosely bound system with a binding energy of 0.762 eV as compared to helium having a binding energy of 24.6 eV. A comparison with DW.CP results shows that PCI affects the capture contribution quite significantly. Figure 1 shows that the DW.CP and DW results are not very different around $\theta_a = 90°$ as opposed to DW.CP.PCI and DW.PCI results

where PCI is included. Another feature we observe that the elimination of PCI leads to an over all reduction in the cross-section, particularly at low energies. As the energy increases all the four results tend to merge into each other.

4 Conclusions

The angular distribution of TDCS at low energies in the case of H^- is found to be very different from the corresponding situation in the helium case. The cross-section shows peaks $\theta_a \approx 30°$ and 150°. This peak decreases with increasing energy. The capture process, in which the incident electron is captured and the two initially bound target electrons are ejected, is found to contribute quite a bit to the TDCS around $\theta_a = 90°$. This process is found to be supported by the PCI.

This work is supported by the Council of Scientific and Industrial Research, Government of India and All India Council for Technical Education. One of us (RKC) would like to thank the University Grants Commission for the award of a research fellowship.

References

1. P. Selles, A. Huetz, J. Mazeau, J. Phys. B **20**, 5195 (1987)
2. P. Schlemmer, T. Rosel, K. Jung, H. Ehrhardt, Phys. Rev. Lett. **63**, 252 (1989)
3. P. Selles, J. Mazeau, A. Huetz, J. Phys. B **23**, 2613 (1990)
4. T. Rosel, R. Bar, K. Jung, H. Ehrhardt, *European Conf. on (e, 2e) collisions and related problems*, edited by H. Ehrhardt (Universitat Kaiserslautern, Kaiserslautern, Germany, 1989), pp. 69-81
5. M. Brauner, J.S. Briggs, H. Klar, J. Phys. B **22**, 2265 (1989)
6. M. Brauner, J.S. Briggs, H. Klar, J. Phys. B **24**, 287 (1991)
7. J. Berakdar, J.S. Briggs, Phys. Rev. Lett. **72**, 3799 (1994)
8. J. Berakdar, Phys. Rev. A **56**, 370 (1997)
9. Z. Chen, Z. Ni, Q. Shi, K. Xu, J. Phys. B **1**, 3803 (1998)
10. S. Jones, D.H. Madison, Phys. Rev. Lett. **81**, 2886 (1998)
11. I. Bray, A.T. Stelbovics, Phys. Rev. A **46**, 6995 (1992)
12. I. Bray, D.A. Konovalov, I.E. McCarthy, A.T. Stelbovics, Phys. Rev. A **50**, R2818 (1994)
13. I. Bray, D.V. Fursa, Phys. Rev. A **54**, 2991 (1996)
14. I. Bray, Phys. Rev. Lett. **78**, 4721 (1997)
15. I. Bray, J. Phys. B **32**, L119 (1999)
16. I. Bray, J. Phys. B **33**, 581 (2000)
17. C.W. McCurdy, T.N. Rescigno, D. Byrum, Phys. Rev. A **56**, 1958 (1997)
18. T.N. Rescigno, M. Baertschy, W.A. Isaacs, C.W. McCurdy, Science **286**, 2474 (1999)
19. M. Baertschy, T.N. Rescigno, W.A. Isaacs, X. Li, C.W. McCurdy, Phys. Rev. A **63**, 022712 (2001)
20. N.C. Deb, D.S.F. Crothers, J. Phys. B **34**, 143 (2001)
21. N.C. Deb, D.S.F. Crothers, Phys. Rev. A **65**, 052721 (2002)
22. L. Malegat, P. Selles, A. Kazansky, Phys. Rev. A **60**, 3667 (1999)
23. L. Malegat, P. Selles, A.K. Kazansky, Phys. Rev. Lett. **85**, 4450 (2000)
24. M.S. Pindzola, F. Robicheaux, Phys. Rev. A **57**, 318 (1998)
25. M.S. Pindzola, F. Robicheaux, J. Phys. B **33**, L427 (2000)
26. C. Pan, A.F. Starace, Phys. Rev. Lett. **67**, 185 (1991)
27. C. Pan, A.F. Starace, Phys. Rev. A **45**, 4588 (1992)
28. S. Jones, D.H. Madison, M.K. Srivastava, J. Phys. B **25**, 1899 (1992)
29. T. Rosel, J. Roder, L. Frost, K. Jung, H. Ehrhardt, S. Jones, D.H. Madison, Phys. Rev. A **46**, 2539 (1992)
30. C. Pan, A.F. Starace, Phys. Rev. A **47**, 2389 (1993)
31. C.T. Whelan, R.J. Allan, H.R.J. Walters, J. Phys. France **3**, 39 (1993)
32. C.T. Whelan, R.J. Allan, J. Rasch, H.R.J. Walters, X. Zhang, J. Roder, K. Jung, H. Ehrhardt, Phys. Rev. A **50**, 4394 (1994)
33. S. Gupta, M.K. Srivasatava, J. Phys. B **29**, 323 (1995)
34. F. Rouet, R.J. Tweed, J. Langlois, J. Phys. B **29**, 1767 (1996)
35. J. Roder, H. Ehrhardt, C. Pan, A.F. Starace, I. Bray, D.V. Fursa, Phys. Rev. Lett. **79**, 1666 (1997)
36. S. Jones, D.H. Madison, Phys. Rev. A **62**, 042701 (2000)
37. M.A. Haynes, B. Lohmann, A. Prideaux, D.H. Madison, J. Phys. B **36**, 811 (2003)
38. A. Prideaux, D.H. Madison, Phys. Rev. A **67**, 052710 (2003)
39. J.B. Furness, J.E. McCarthy, J. Phys. B **6**, 2280 (1973)
40. F.A. Gianturco, S. Scialla, J. Phys. B **20**, 3171 (1987)
41. D.A. Biava, K. Bartschat, H.P. Saha, D.H. Madison, J. Phys. B **35**, 5121 (2002)
42. K.D. Winkler, D.H. Madison, H.P. Saha, J. Phys. B **32**, 4617 (1999)
43. D.A. Biava, H.P. Saha, E. Engel, R.M. Dreizler, R.P. McEachran, M.A. Haynes, B. Lohmann, C.T. Whelan, D.H. Madison, J. Phys. B **35**, 293 (2000)
44. S. Jetzke, J. Zaremba, F.H.M. Faisal, Z. Phys. D **11**, 63 (1989)
45. S. Jetzke, F.H.M. Faisal, J. Phys. B **25**, 1543 (1992)
46. A. Becker, S. Jetzke, F.H.M. Faisal, Hyperf. Interact. **89**, 83 (1994)
47. M.R.H. Rudge, Rev. Mod. Phys. **40**, 564 (1973)
48. S. Chandrasekhar, J. Astrophys. **100**, 176 (1944)